Genetic algorithm-based optimization of a multi-stage flash desalination plant

G.N. Sashi Kumar[*], A.K. Mahendra, A. Sanyal, G. Gouthaman

Machine Dynamics Division, CEL-5, Bhabha Atomic Research Centre, Trombay, Mumbai 400085, India
Tel. +91 (22) 2559 3611; Fax: +91 (22) 2550 5151; email: gnsk@barc.gov.in

ABSTRACT

The MSFSIM, a simulator which predicts the performance of a multi-stage flash (MSF) desalination plant, has been coupled with a genetic algorithm (GA) optimizer. The nuclear desalination demonstration project (NDDP) at Kalpakkam, India, has a MSF plant under construction. Exhaustive optimization case studies have been conducted on this plant with an objective to increase the performance ratio (PR) and minimize the start-up time. The steady-state optimization performed was targeting the best stage-wise pressure profile to enhance thermal efficiency which, in turn, improves the performance ratio. Apart from this, the recirculating brine flow rate was also optimized. This optimization study enabled us to increase the PR of the NDDP–MSF plant from a design value of 9.0 to an optimized value of 13.1. A further increase of 20% in the heat transfer area, extra area provided for seasonal variation, has taken the PR to 15.1 under optimized conditions. A desire to maintain equal flashing rates in all of the stages (a feature required for long life of a MSF plant) has also been achieved. The deviation in the flashing rates within stages has been reduced. The start-up variation behavior of the plant was also optimized using MSFSIM coupled with the GA optimizer. This study minimized the start-up time to reach the optimized steady state.

Keywords: Optimization; MSFSIM; NDDP; MSF; Performance ratio; Genetic algorithm; Start-up

1. Introduction

In India, a nuclear desalination demonstration plant (NDDP) is under construction at Kalpakkam, Tamil Nadu, India, with a design capacity to produce 4500m^3/d of potable water from seawater. A pilot plant (capacity of 425 m^3/d, Bhabha Atomic Research Centre, Trombay, Mumbai) of performance ratio (PR) of 9.0 was constructed, commissioned and successfully run to understand the process of nuclear desalination. (Performance ratio is defined as the ratio of kilogram of potable water produced per kilogram of steam consumed). These pilot plant data [1] have been used in the design of the NDDP MSF plant [2]. Optimization of the NDDP MSF plant is carried out for two reasons, namely (a) maximization of PR and (b) minimization of variation of flashing rates in

all the stages. Start-up optimization was also performed. A numerical simulator (MSFSIM) was developed based on mathematical modeling to aid the control systems in the plant [2–5]. This has features for troubleshooting and can aid in the training of the operators. This simulator was validated using the pilot plant data.

In this paper the optimization of various possible parameters in the NDDP MSF plant to enhance its performance ratio has been discussed. MSFSIM has been coupled with the genetic algorithm optimizer. Primary parameters like (1) the stage-wise pressure profile and (2) the recirculation flow rate are parameterized while the secondary parameters like reject and blow down are adjusted by the simulation code, MSFSIM, so as to maintain thermal and concentration balance. The best operating parameters have been reported in this paper.

Section 2 of the paper discusses the mathematical modeling and validation with respect to the pilot plant.

*Corresponding author.

Section 3 gives the details of the optimization study and elaborates the results suggesting the optimal zone of operation. Section 4 gives the details of start-up optimization, followed by the future scope and conclusions.

2. Validation and problem definition

The MSF plant consists of a brine heater and evaporators which are arranged in series. The flow sheet in Fig. 1 shows the arrangement of evaporators in the recovery and the reject stages for the NDDP MSF plant. The basic model equations [1] have been listed in the Appendix. The correlations used for physical properties like density, viscosity, etc. of the brine are listed in the Appendix. Asteam table has been coded and used to determine all the properties of the vapor. Further details can be had from reference [6]. Fig. 2 gives the flow diagram for a typical brine evaporator.

The thermal efficiency of the flashing chamber is assumed to be 99%. Non-equilibrium allowance has been given to the system [7]. The steam supplied to the brine heater was taken as saturated. It is also assumed that the vapor in the evaporator attains equilibrium with the liquid in contact instantly.

The multi-stage flash desalination process can be described by a system of ordinary differential equations (ODEs) mentioned in the Appendix. Dynamic model equations were used so that steady state and transient (start-up) can be modeled with the same set of equations. The numerical simulator, MSFSIM, solves these ODEs simultaneously using the Runge–Kutta (RK) four-time stepping. The steady-state simulations use pseudo-time stepping, with a large time step to enhance faster convergence, whereas in transient simulations explicit time marching was implemented in the outer time cycle (after being stabilized with Gauss–Seidel inner iterations). The steam flow rate is constant during the study; also the brine level inside the evaporators is taken equal to the weir height throughout the stage length. For utilizing this simulator for training purposes, a graphic user interface (GUI) was also developed [4,5]. The validation of this MSFSIM was done with data from the pilot plant with 30 recovery stages and three reject stages. It had a capacity of 425 m³/d. The process details of the pilot plant are listed in Table 1 [4,5].

2.1. Validation with pilot plant data

The data from the pilot plant under normal operating conditions are compared with the simulated data from MSFSIM in Table 2. Figs. 3 and 4 shows a comparison of temperatures and production rate under startup condition
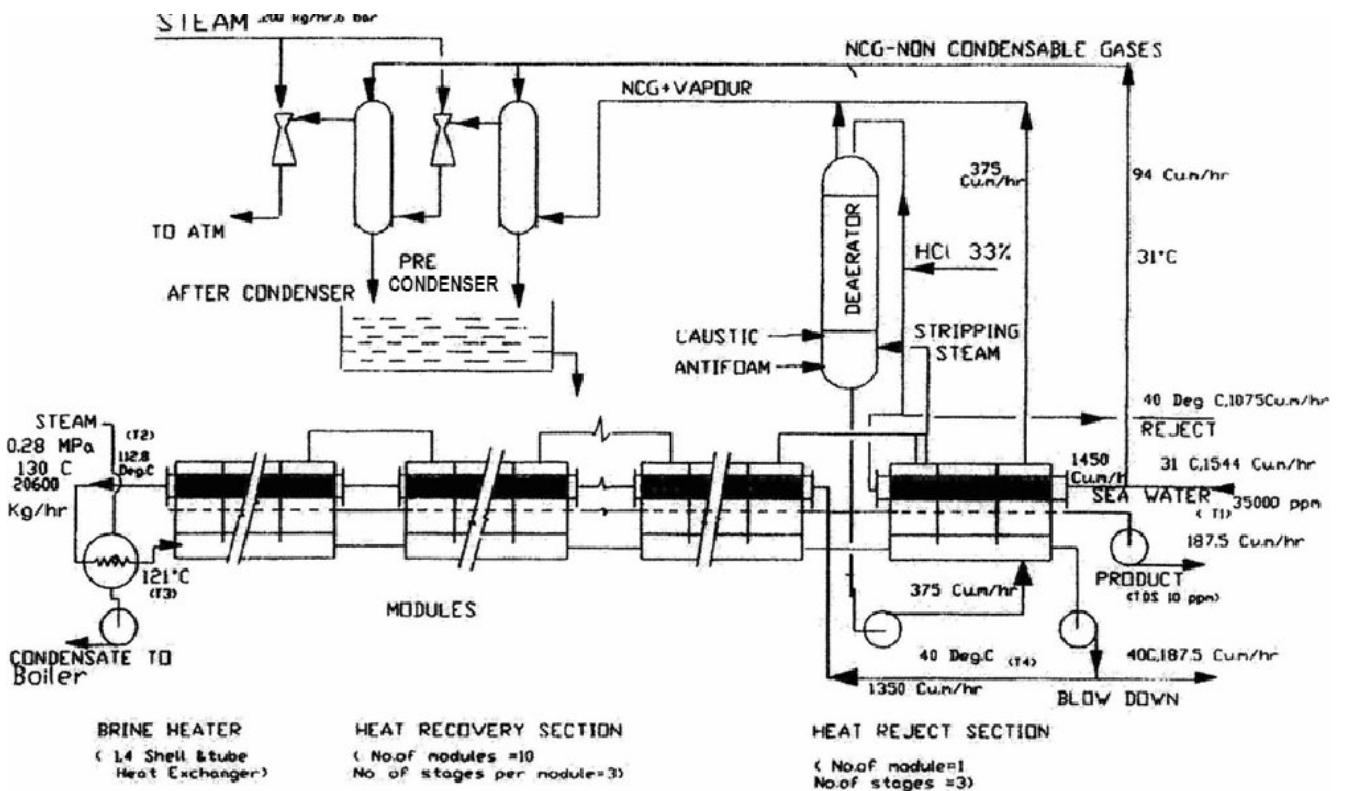
Fig. 1. NDDP MSF desalination flow sheet with design rating 4500 m³/d.
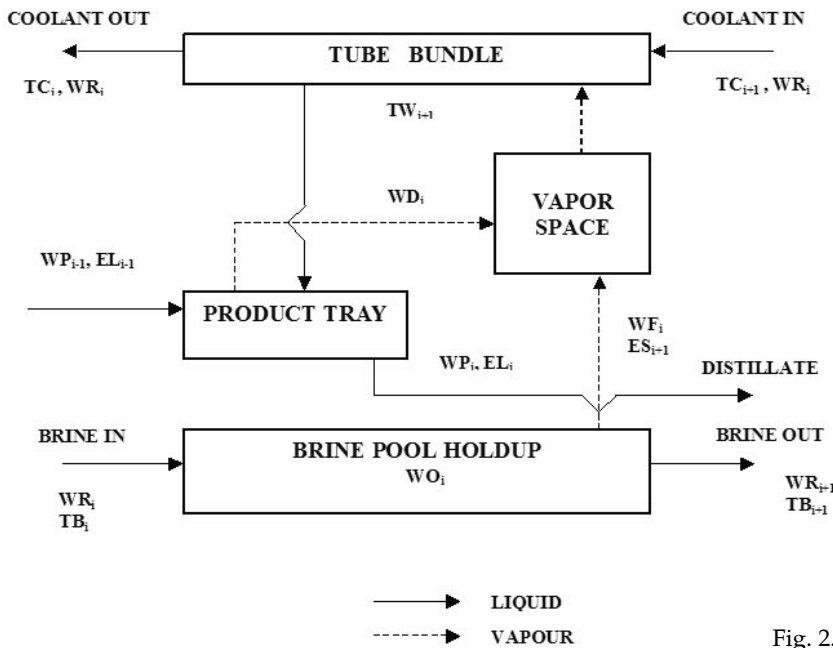
Fig. 2. Flow diagram for a typical i^{th} evaporator.
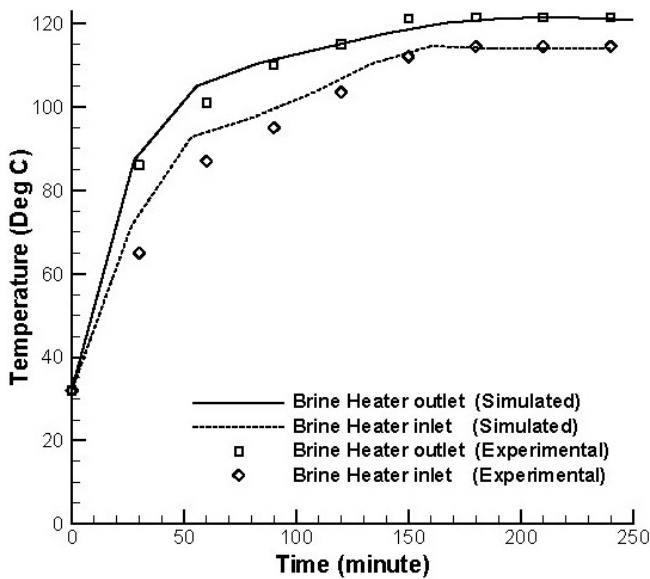
Fig. 3. Development of brine heater temperatures compared with pilot plant data.
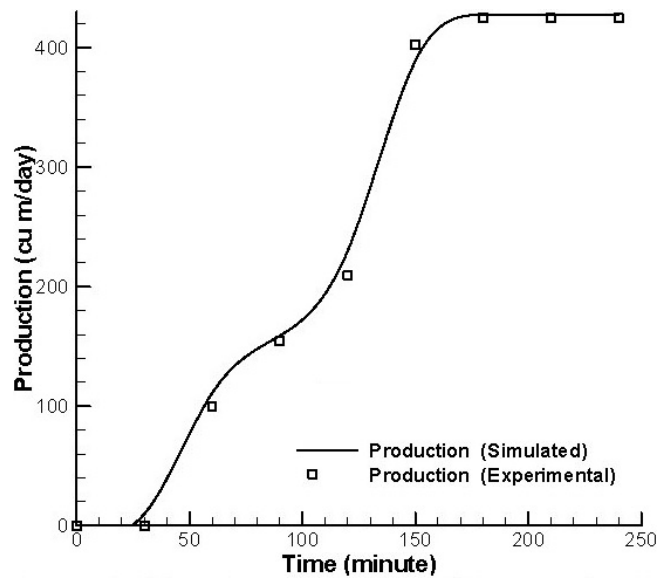
Fig. 4. Development of production rate compared with pilot plant data.

with the pilot plant data. A time step of 0.01 min was used in the numerical calculation. For further details please refer to BARC reports [4,5]. The systems of equations to be tested were given an impulse and step inputs and the stability of the solver were tested. The inputs tested were recirculation flow rate, steam mass flow rate/temperature, pressure in a few stages and salinity of seawater/temperature. The solver has converged for all the cases for which testing was conducted. Figs. 5 and 6 show step inputs of steam and recirculation flow rates and its response from the NDDP–MSF plant simulator.

The MSFSIM code was extensively validated with the data of a 425 m^3/d capacity pilot plant located at Trombay, Mumbai. The numerical residue in the material and energy balance of the code is of the order of 10^{-4}%. Table 3 gives the cross-correlation coefficient as well as the least-squares error for brine heater inlet, outlet and the production rate in comparison with the experimental data as shown in Figs. 3 and 4.

It can be seen that MSFSIM compares well with the pilot plant data. Having validated the MSFSIM process simulator, the process optimization is carried out, as discussed in the next section.

Table 1
Process parameters of the pilot plant at Trombay and the NDDP MSF at Kalpakkam

Parameters	Pilot plant, Trombay	NDDP MSF plant, Kalpakkam
Distillate production rate (m³/d)	425	4,500
Number of recirculation/reject stages	30/3	36/3
Feed water flow rate (m³/h)	90.5	1,450
Brine heater inlet temperature (°C)	113.0	112.8
Brine heater outlet temperature (°C), TBT	121.0	121.0
Performance ratio	9.0	9.0
Blow down salinity (ppm)	52,000	70,000
Blow down flow rate (m³/h)	35.0	187.5
Blow down temperature (°C), BBT	44.0	40.0
Rejection flow rate (m³/h)	38	1,075
Rejection temperature (°C)	40	40

Table 2
Comparison of the simulated data with the pilot plant data

Parameters	Pilot plant data	Simulated by MSFSIM
Distillate production rate (m³/d)	425	430.52
Brine heater inlet temperature (°C)	113	114.07
Brine heater outlet temperature (°C), TBT	121	121.3
Performance ratio	8.92	9.03

Table 3
Comparison of the start-up with the experimental data

Parameter	Cross correlation	Least-square error, %
Brine heater inlet temperature (Fig. 3)	0.9913	5.53
Brine heater outlet temperature (Fig. 3)	0.9972	2.46
Production rate (m³/d) (Fig. 4)	0.9988	4.87

2.2. Performance of the NDDP MSF plant at the design condition

The accuracy and validity of the MSFSIM (steady-state and start-up) solvers can be seen from the above-mentioned validation of MSFSIM against the pilot plant data. The performance of the NDDP MSF plant using MSFSIM was predicted. This plant contains 39 stages (36 recovery, three reject), with brine concentration ratio (BCR) operating at 2.0. (BCR is the ratio of the salinity of
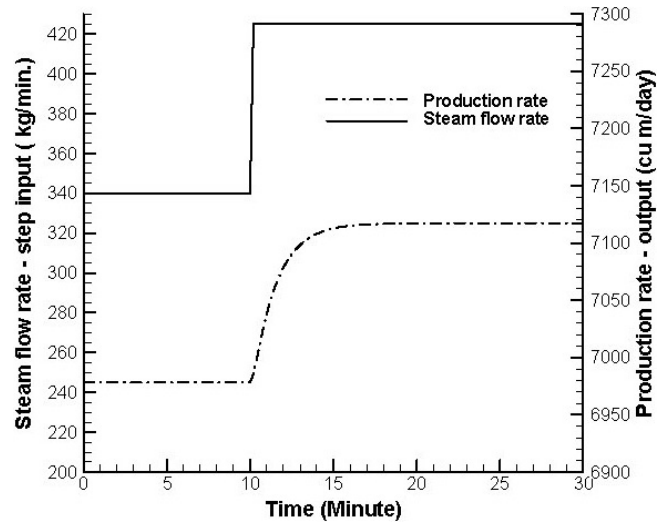
Fig. 5. Response of production rate for a step input in steam flow rate in the NDDP MSF plant.
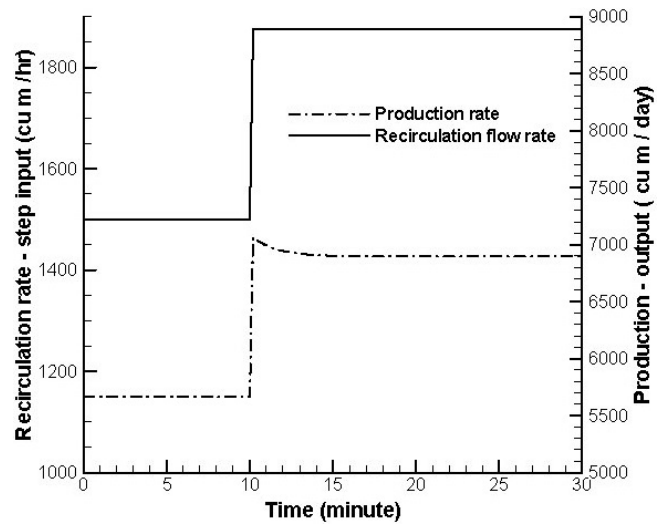
Fig. 6. Response of production rate for a step input in recirculation flow rate in the NDDP MSF plant.

blow down to feed water salinity). The design velocity for the recircul-ating brine in stage number 1 was fixed at 1.2 m/s [8], thus the recirculating brine flow rate is fixed at 1,350 m³/h. Fig. 7 gives the flashing rates in all the stages under design condition for the NDDP MSF plant. The process details of the NDDP MSF plant are listed in Table 1 [4,5].

2.3. Motivation for optimization

Variation of recirculation flow rate reveals the non-optimality of the design data. An increase in recirculating brine (here onwards referred as RB) flow rate alone increases the PR from a design value of 9.0 as reported previously [8] to 10.81. Flashing is very strongly dictated
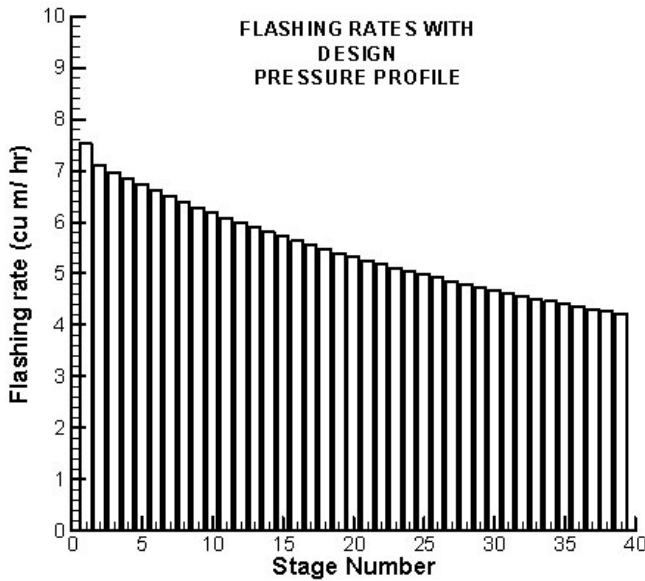
Fig. 7. Stage-wise flashing rates at design condition.

by the stage pressures. Optimal variation of stage pressure not only increases PR but can also minimize the variation amongst stage flash rates.

Equal flashing in all stages is a desired feature for having a long-running plant, but the design condition does not provide this. It gives an average deviation of 0.8935 m^3/h from the mean value of flash as shown in Fig. 7. A better optimum should definitely exist for this plant in terms of the operating conditions. The parametric space of interest was explored for reaching the optimum.

3. Optimization using a genetic algorithm— steady-state simulation

Genetic algorithms are search algorithms based on natural selection and genetics. They combine survival of the fittest among the string structures with a structured yet randomized information exchange. In every generation, a new set of strings is created using bits and pieces of the fittest individuals of the older generation; an occasional new part is tried to maintain diversity. They efficiently exploit historical information to improve the performance [9].

3.1. Problem definition and the optimization procedure

The optimization in this context requires maximization of PR and minimization of average variation of the flashing rates (m^3/h), σ in all the stages, defined as

$$\sigma = \left[\frac{1}{2}\sum_{i=1}^{39}\left(f_i - \overline{f}\right)\right]^{1/2}$$

where f_i is the flashing in stage i and $\overline{f}$ is the average flashing in all stages. An optimization problem can be mathematically stated as follows:
Find

$$\vec{x} = \begin{bmatrix} x_1 \\ x_2 \\ \vdots \\ x_n \end{bmatrix} \text{ which maximizes/minimizes OF}_i(\vec{x})$$

subject to inequality/equality constraints

$$g_j(\vec{x}) \le 0 \qquad j = 1, 2, .., m$$

$$h_j(\vec{x}) = 0 \qquad j = 1, 2, ..., p$$

where $\vec{x}$ is an n-dimensional design/control vector. In the present case the vector space is the stage pressures and the brine recirculation flow rate of a MSF plant, i.e. this vector space $\vec{x}$ =[P_1, P_2, ..,P_{39}, recirculation brine flow rate]^T. The first step is the parameterization of the design/control vector and the second most important step is to condense this vector space to a smaller dimensional space. The pressure profile variation is non-linear with respect to stage whereas the T_s, saturation temperature varies quite linearly with respect to stage. Thus, the T_s curve is parameterized instead of the stage pressure. The vector space is further condensed by fitting a cubic spline with seven control parameters.

The inequality constraint defines the operating region of the designed plant. They are TBT $\le 121\,°C$, BBT $\ge 40\,°C$, $f_i \ge 0.0$, $1.0\,\text{m/s} \le V_{RB,Max} \le 1.6\,\text{m/s}$ and $S_{BD} = 70,000$ ppm.

This can be cased in a vector format as follows:

$$g(\overline{x}) \equiv \begin{bmatrix} \text{TBT} - 121\,°C \\ 40\,°C - \text{BBT} \\ -f_i, i = 1, 2, ..., 39 \\ |\,V_{RB,Max} - 1.3\,| - 0.3\,\text{m/s} \end{bmatrix} \le 0$$

and

$$h(\overline{x}) \equiv \begin{bmatrix} S_{BD} - 70,000\ \text{ppm} \end{bmatrix} = 0$$

where $V_{RB,Max}$ is the maximum velocity of the recirculating brine inside the tubes and S_{BD} is the blow down salinity. The pumping limits of various pumps in the circuit gets determined by the limits of $V_{RB,Max}$.

Any change in the recirculation flow rate affects the reject, blowdown and seawater inlet flow rates. The optimization zone is within the pumping capacities of the installed pumps. The parameter of much concern to us is the maximum velocity of brine inside the tubes. If the maximum velocity in brine tubes is within the permissible limits (limits decided as per salinity to minimize fouling,

CaSO$_4$ deposition). The stage pressure is bounded between the pressure in the first stage based on the TBT and the last stage based on the BBT. Hence the intermediate stage pressures are optimized.

There are multiple objectives, multiple constraints. The concept of Pareto optimality has been taken as the basis for the cooperative multiple objective optimization. This uses the dominance strategy where an optimum $\vec{x}^*$ is said to dominate $\vec{x}$ if and only if

$$\begin{cases} \forall\ i\ \in \{1,2,...n\},\ OF_i(\vec{x}^*) \leq OF_i(\vec{x}) \\ \exists\ i\ \text{such that}\ OF_i(\vec{x}^*) < OF_i(\vec{x}) \end{cases}$$

This $\vec{x}^*$ is said to be non-dominated if there is no feasible solution in the search space that dominates it. The Pareto front is a set of all such non-dominated solutions.

It is a challenging task to design an appropriate (1) parameterization, (2) binary coding of parameter set and (3) objective function that can evolve to the global optimum using a GA. An inappropriate handling of constraints may lead to a local optimum of the problem. It should be noted that stability of optimization state is also of equal concern.

Fig. 8 is the schematics of the optimization study. An optimization study using a downhill simplex method was tried earlier. The optimum obtained using this method was always very close to the initial guess chosen and good increase in objective function was not achieved. Probably the method gets struck in the local optimum close to the initial guess. It was decided to try a population-based method to get a global optimum. There are many population-based methods, namely simulated annealing (SA), genetic algorithm (GA), ANT algorithms, etc. Out of these GA and SA have been extensively reported for determining the Pareto set of optimization. Earlier experience with GA [10,11,13] has made it the obvious

choice for this problem. GA searches from multiple vectors in the design space simultaneously and stochastically, instead of moving from a single point deterministically like in gradient-based methods. This feature prevents optimal candidates from settling in a local optimum. Moreover, GA does not require computing gradients of the objective function [10,11,13]. These characteristics lead to the following three advantages of GA:

- GA has the capability of finding global optimal solutions.
- GA can be processed in parallel.
- MSF design and analysis codes can easily be adapted to GA without any modification because GA uses only objective function values.

Fig. 9 shows the schematic of the procedure used for coupling MSFSIM with GA. GA works on a coding of the design variables subject to the defined performance constraints.

Fig. 10 shows a typical chromosome (gene) structure. It contains nine parameters, each coded as 15-bit binary code and concatenated to form a single string. Fig. 11 shows a typical saturated temperature (T_s) profile in various stages. The stage pressure is determined as a function of T_s. The T_s curve is parameterized as shown in Fig. 11. As explained earlier, this is achieved by fitting a cubic spline with the seven control parameters. Cubic spline with seven control parameters does not regress the saturated temperatures of the 39 stages. Here it is used to ensure inter-stage smoothness; otherwise there can be drastic jumps and discontinuities in the saturated temperature between stages. Such a discontinuous pressure/temperature profile leads to unrealistic/unimplementable conditions. In order to meet the first constraint of the top brine temperature (TBT) <121°C, saturated temperature for the first stage is taken to be constant at 117.2°C. The vacuum system available in this plant has a constraint on the bottom brine temperature (BBT) >40°C. Thus, the saturated temperature for the 39th stage was chosen to be constant 39.5°C.

Each of the seven control points (CP_i) for the T_s curve vary as the percentage of the initial (design) value (see Fig. 11). Even though spline smoothens the inter-stage saturated temperature, in real life there are small discrete jumps in the inter-stage saturated temperatures. Numerically the correction based on log mean temperature difference (LMTD) is introduced to bring a local discreteness in the saturated temperature profile.

Fig. 12 shows a typical temperature profile of recirculating brine in the stage. A change in the pressure profile and recirculating flow rate leads to change in LMTD in all the stages. It should be noted that for higher values
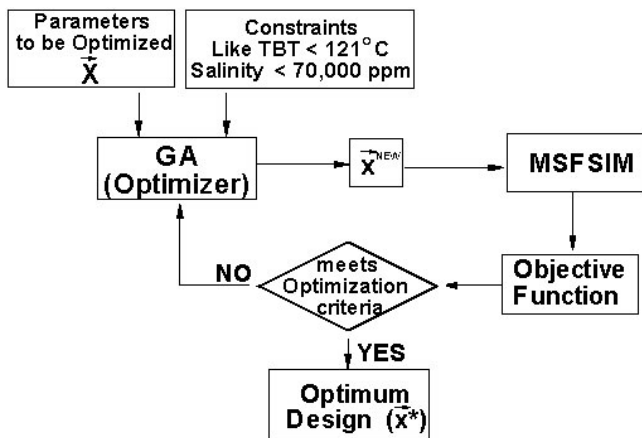
Fig. 8. Schematics of the genetic algorithm MSF optimizer.
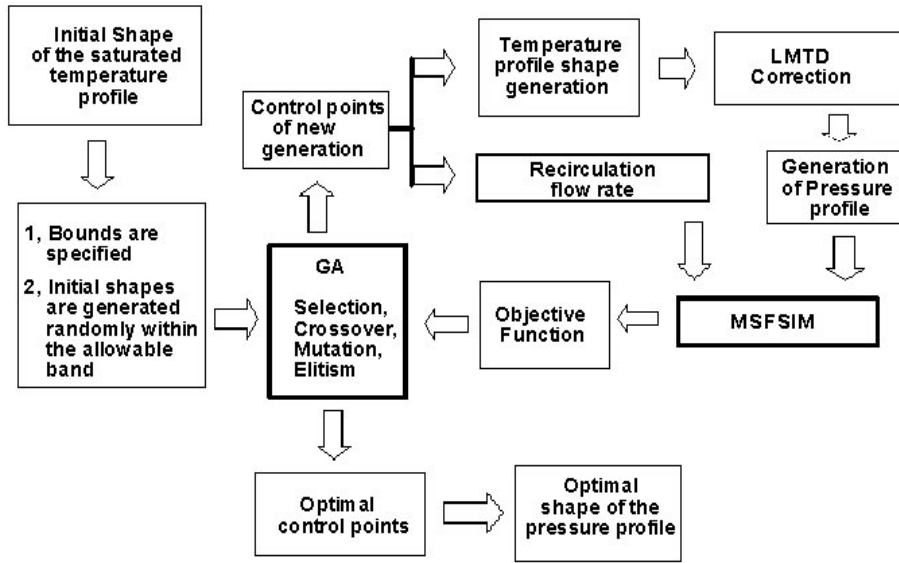
Fig. 9. Schematics showing the procedure of coupled MSFSIM with GA.

```
Parameter    Binary code of 1ˢᵗ parameter     Binary code of 2ⁿᵈ  parameter
number
           ⎧‾‾‾‾‾‾‾‾‾‾‾‾‾‾‾‾‾‾‾‾‾‾‾⎫ ⎧‾‾‾‾‾‾‾‾‾‾‾‾‾‾‾‾‾‾‾‾‾‾‾⎫
1, 2        1 0 0 1 1 0 0 1 1 0 1 0 1 0 0 0 0 0 1 0 1 1 0 0 1 1 1 0 1 1
3, 4        0 0 1 0 0 0 1 1 0 0 1 0 1 0 0 1 1 1 0 0 1 0 0 1 1 0 0 0 0 1
5, 6        0 0 1 1 1 1 1 1 0 1 1 0 1 0 0 0 1 1 1 0 0 0 0 0 0 1 1 0 0
7, 8        1 0 1 1 0 0 0 1 1 1 0 1 0 0 1 0 0 1 0 1 1 0 0 0 1 0 0 0 0 0
9           0 1 0 1 0 1 1 1 0 0 1 0 1 0 1
```

Fig. 10. Typical chromosome for the control parameters chosen.
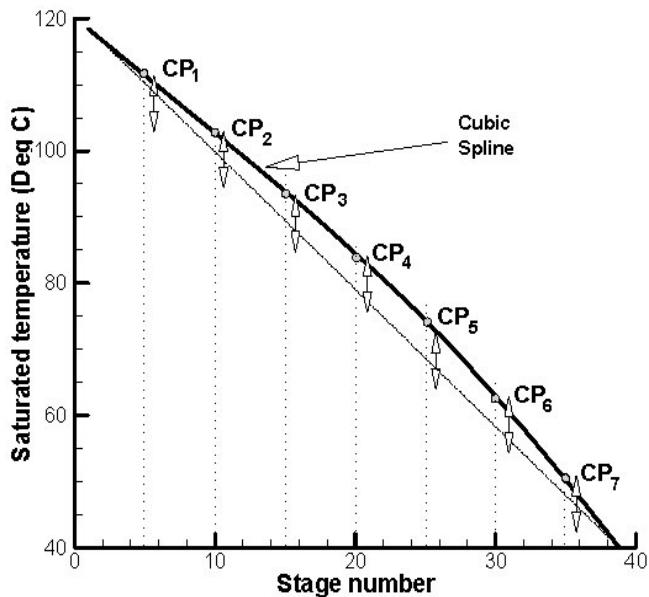
Fig. 11. Typical curve showing the temperature vs. stage number plot.

of LMTD the performance improves. Any correction for the T_s curve based on the LMTD at a fixed recirculation flow rate will change the vapor space temperature thereby fixing the stage pressure. The value of T_s for each stage is readjusted using the following equation:

$$T_s\big|_{\text{Stage } i} = T_s\big|_{\text{Stage } i}^{|\text{From spline}}$$

$$+ \left(LMTD\big|_{\text{Mean}}^{\text{Reference}} - LMTD\big|_{\text{Stage } i}^{\text{Reference}} \right)$$

$$\times \frac{LMTD\big|_{\text{Stage } i}}{LMTD\big|_{\text{Mean}}} \times \Psi$$

This adjusts the stage pressure such that the LMTD of each stage approaches the mean LMTD. The Ψ factor brings the discreteness in the stage pressure profile. This forms the 8th parameter for the optimization. The LMTD for all stages is calculated and stored for the elite member in the previous generation. This forms the reference set for LMTD$_{\text{Mean}}$ and LMTD$_{\text{Stage } i}$.
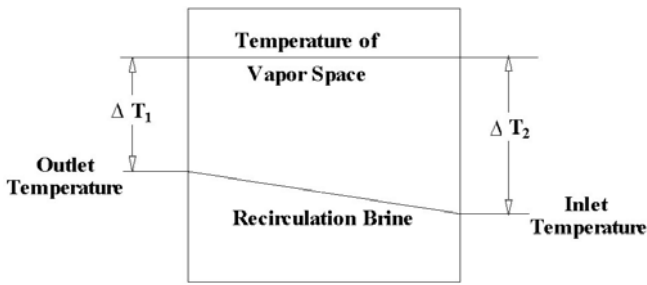
Fig. 12. Typical recirculating brine temperature profiles.

Table 4
Initial input range for GA

Control parameter	Mean value	Range, %
CP_1 (control point at stage =5)	108.84	−7 to +7
CP_2 (control point at stage = 10)	98.645	−8 to +8
CP_3 (control point at stage = 15)	88.447	−9 to +9
CP_4 (control point at stage = 20)	78.250	−10 to +10
CP_5 (control point at stage = 25)	68.053	−11 to +11
CP_6 (control point at stage = 30)	57.855	−12 to +12
CP_7 (control point at stage = 35)	47.658	−13 to +13
CP_8 (Ψ factor based on LMTD)	0.0	−30 to +30
CP_9 (RB flow rate)	1463	−23 to +23

A ninth parameter is also used for optimization, which is the recirculation flow rate. In this analysis, a given population represents a number of configurations with different T_s (or) pressure profiles, a factor for LMTD correction and various recirculation flow rates. Thus each configuration is regarded as a single chromosome. The initial guess of the control parameters is randomly generated. All the parameters are allowed to vary within a band as shown in Table 4 and Figs. 13 and 14. The population size is set to 16. The fitness evaluation is the basis for GA search and selection procedures. GA aims to reward individuals (chromosomes) with high fitness values (more fit for reproduction) and to select them as parents to reproduce offspring. The purpose of optimization in this study is to increase the PR of the MSF plant. This value of fitness is determined by using a suitable objective function (OF). The fitness is chosen to be same as the objective function which is defined as

$$OF = \alpha \left(OF_1 \right) + \beta \left(OF_2 \right)$$

where the first objective function is $OF_1 = PR$ and the second objective function is

$$OF_2 = \frac{1}{\text{Max} \left\{ \sigma, 0.5 \right\}}$$

where α and β are the weights for the Pareto optimality,
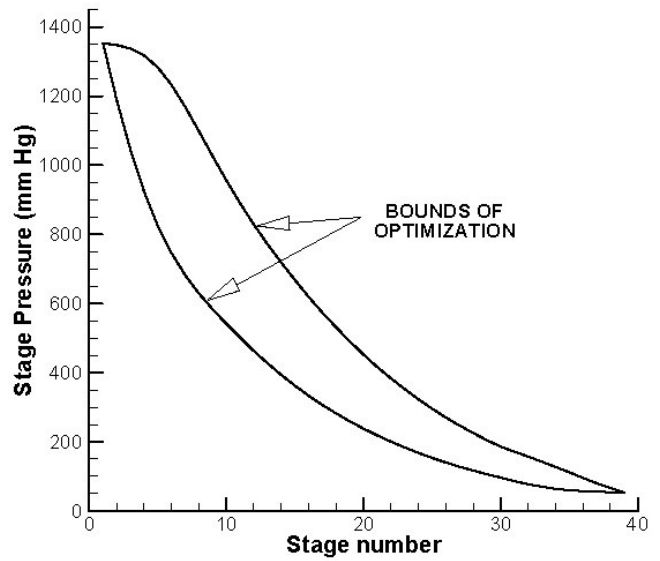
Fig. 13. Search space for the optimization of the pressure profile.
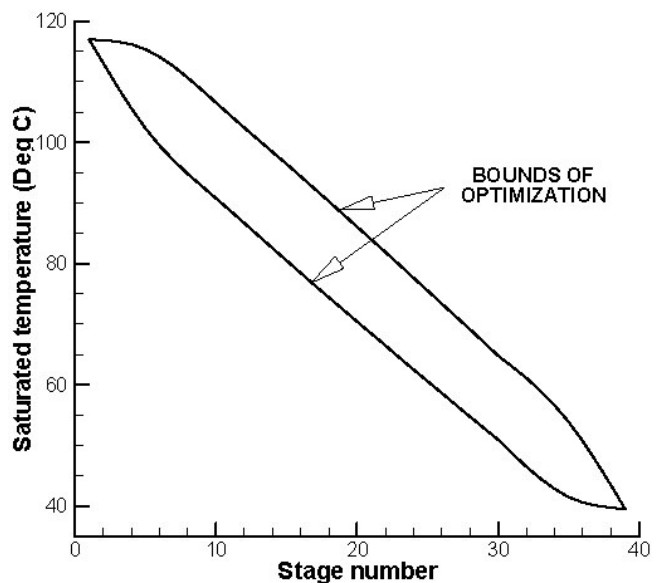
Fig. 14. Search space for the optimization of the T_s profile.

PR is the performance ratio of the MSF plant and σ is the average variation of the flashing rates (m³/h) in all stages. The function Max{σ,0.5} facilitates the value of σ to approach 0.5 (which would be acceptable for the real plant). This, in turn, enables us to achieve almost equal flashing in all of the stages. Numerical experimentation was done giving more importance for σ (i.e. low α and high β), which resulted in low value of σ, ~0.1 m³/h, but the PR was as low as ~11.5, which was not acceptable. Similarly, when high α and low β were used, the PR was ~13.1 and σ was unacceptable: ~1.2 m³/h. The approach used is called "minimizing/maximizing weighted sums of
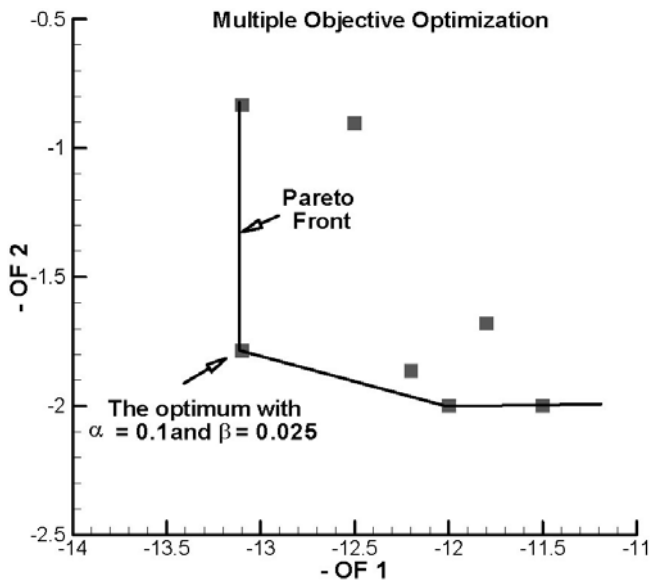
Fig. 15. Pareto front and the choice of α and β.

Fig. 16. Evolution of highest fitness candidate with generation.

functions". We have constructed the Pareto front for this multi-objective optimization problem. Fig. 15 shows the Pareto front; the dots represent various optimum solutions obtained with different sets of values for α and β. The best of the Pareto optimum, shown as a line in Fig. 15, was chosen to determine the values of α and β. Hence α = 0.1 and β = 0.025.

This multi-objective function (*OF*) increases the PR as well as reduces the variation in flashing rates in all the stages. The MSFSIM calculates the PR with the pressure profile and recirculation rate provided and sends them to GA, which uses this formula to obtain the *OF*, which is a measure of fitness of that configuration (parameters). The design conditions were used as the initial optimization conditions. For each member in the population, one *OF* evaluation is needed; MSFSIM has to run for each configuration. Parents are chosen based on the tournament method [9]. In this method a fictitious tournament is held among the members of the same generation. Only the winning parents (having high value of fitness) are chosen and allowed to reproduce. Each pair of parents produces two offspring (chromosomes) by crossover. The uniform crossover scheme is applied. The probability of the crossover is set at 90%. Then, mutation is applied to the offspring. Mutation was carried out by randomly selecting a gene (control node) and changing its value by an arbitrary amount within a prescribed range, as illustrated in Figs. 13 and 14. A new set of population is thus produced.

The best members in each generation are assigned to the next generation without crossover or mutation [9]. This technique, known as elitism, guarantees that the best member in all the populations will not be filtered out as
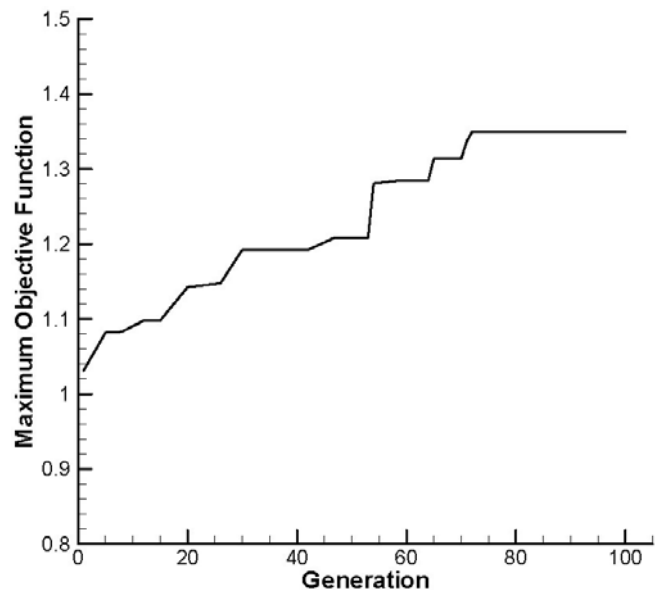
the optimization proceeds. The optimization continues till the *OF* vs. generation curve saturates. The highest *OF* contributing member would be the optimum solution to the problem.

3.2. Results and discussion

Our previous research experience using a GA-based optimizer [10,11,13] has helped in choosing the parameters that will be used within GA (Table 5). Fig. 16 gives the evolution of the objective function with the generation, which saturates after 116 generations, the details of the optimum is given in Table 8. The optimized sets of parameters are given in Table 6. Here PR reaches a value of 13.12 when the optimized recirculation flow rate is around 1795 m^3/h.

Fig. 18 shows a comparison between the design and optimized pressure profile. Fig. 17 shows the flashing rates in various stages with optimized pressure and recirculation flow rates.

3.3. Possibility for optimum

The recirculating brine that is preheated in the evaporator stages is the most critical part of the MSF plant and has a role to play in our optimum design. The LMTD for a given recirculating brine in each stage is calculated. The recirculation flow rate used is also higher in the optimized case. As expected, the sum of LMTD in all the stages for optimized case is higher than the design case.

Fig. 19 confirms our conclusion that LMTD in many stages has improved due to the optimum pressure profile
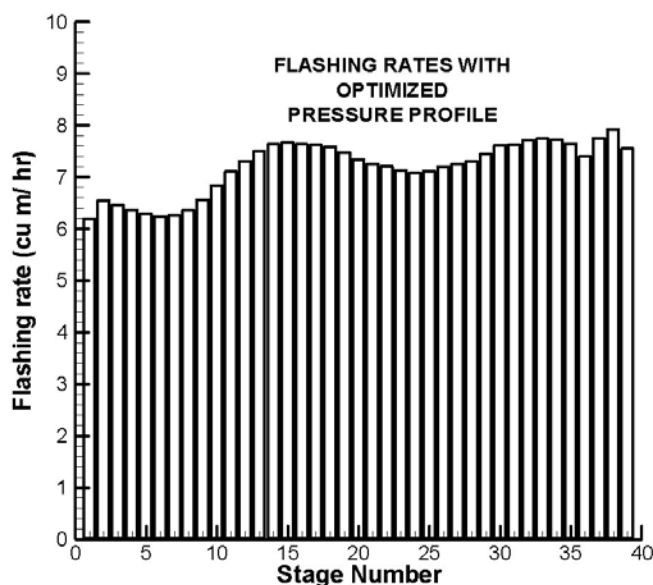
Fig. 17. Flashing rates in stages under optimized condition.
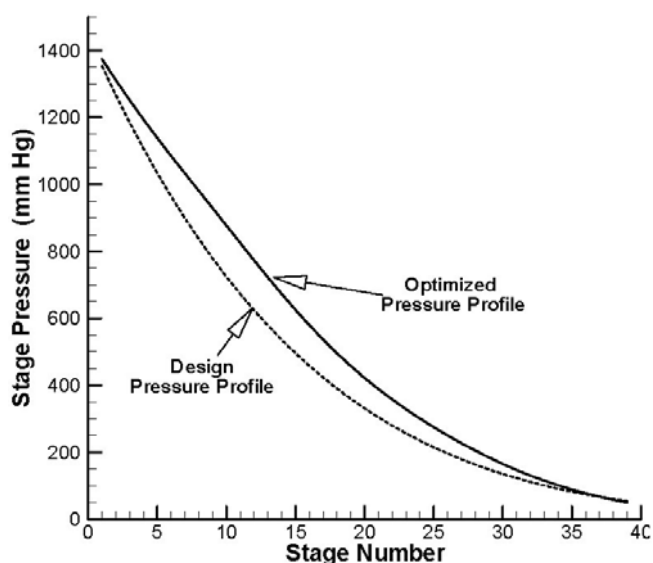
Fig. 18. Comparison of optimized and design (initial) pressure profile.

along with an appropriate increase in recirculation flow rate. The average LMTD increases from 4.33 °C (design) to 5.07 °C (optimum case). The comparison of vapor temperature in various stages for the design and optimum case is shown in Fig. 19. Fig. 20 shows the comparison between design and optimum for recirculating brine inlet and outlet temperatures.

During the process of optimization the temperature of the vapor space changes as a consequence of the pressure change. Similarly an increase (or decrease) in recirculation flow rate changes the ΔT_1 and ΔT_2 as shown in Fig. 11. Thus the optimum pressure profile and recirculation flow

Table 5
Parameters of GA

Population size	16
Max. number of generation	130
Number of bits per parameter	15
Crossover probability	0.9
Jump mutation probability	0.2
Creep mutation probability	0.05

Elitism used
Tournament selection used
Uniform cross over used

Table 6
Optimized parameters set obtained

Parameter	Differential value, %	Actual value
CP_1 (control point at stage = 5)	2.36	111.410
CP_2 (control point at stage = 10)	5.54	104.110
CP_3 (control point at stage = 15)	7.35	94.950
CP_4 (control point at stage = 20)	8.38	84.809
CP_5 (control point at stage = 25)	9.55	74.552
CP_6 (control point at stage = 30)	9.51	63.360
CP_7 (control point at stage = 35)	6.03	50.532
CP_8 (Ψ factor on LMTD)	28	0.28
CP_9 (RB flow rate)	21.3–22.7	1775–1795
PR	12.86–13.12	

Table 7
Comparison of LMTD under design and optimized conditions

	Design condition	Optimized condition
$\sum_{i=1}^{39} LMTD$, °C	168.7	197.9
RB flow rate, m³/h	1350	1785

Table 8
Details of the optimized steady solution

Description	MSF at design condition	MSF at optimized condition
Capacity, m³/d	4,500	6,480–6,595
TBT, °C	121.0	120.17–120.31
RB flow rate, m³/h	1,350	1,775–1,795
Brine heater temp. rise, °C	8.2	6.33–6.25
Performance ratio	9	12.86–13.12
Average deviation of flashing in all stages	0.894	0.537–0.553
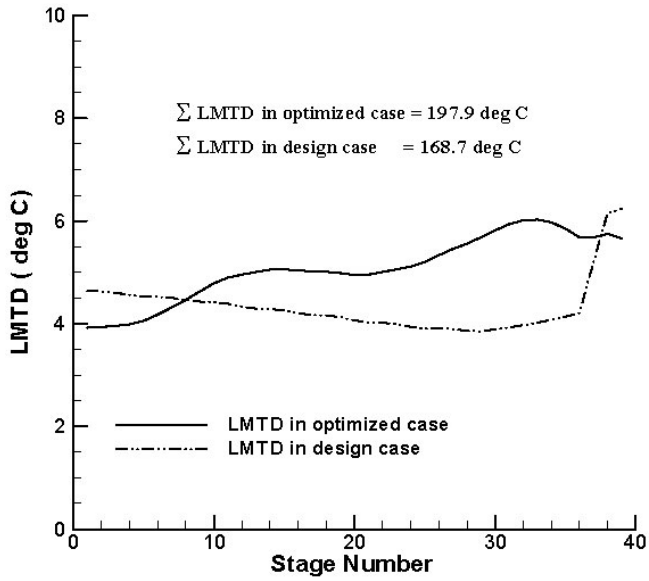
Fig. 19. LMTD for the design and optimized cases for all stages.
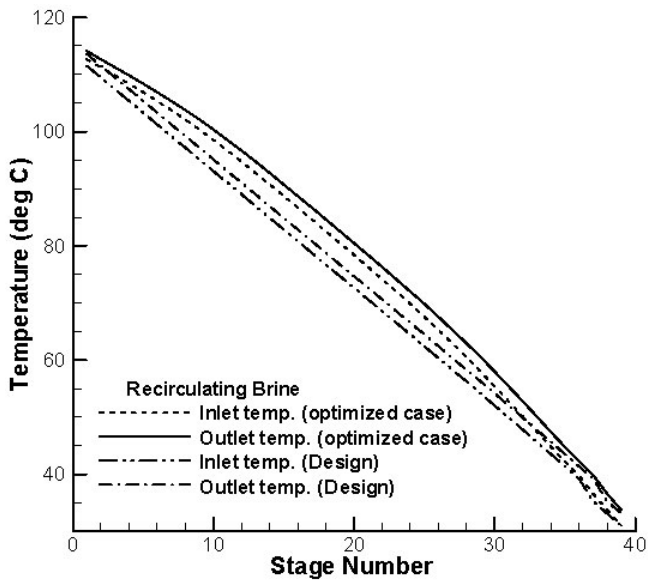
Fig. 20. Inlet and outlet temperatures of the RB for design and optimized cases for all stages.

rates lead to a higher LMTD in all the stages (i.e., higher $\sum_{i=1}^{39} LMTD$). Thus the temperature gained in the recirculation section is directly proportional to the $\sum_{i=1}^{39} LMTD$.

Table 7 gives the details of the optimized condition in comparison with the design condition. Fig. 21 shows the comparison between design and optimum PR as a function of recirculating brine flow rate. It shows a sharp drop in PR when the RB flow rate crosses a threshold
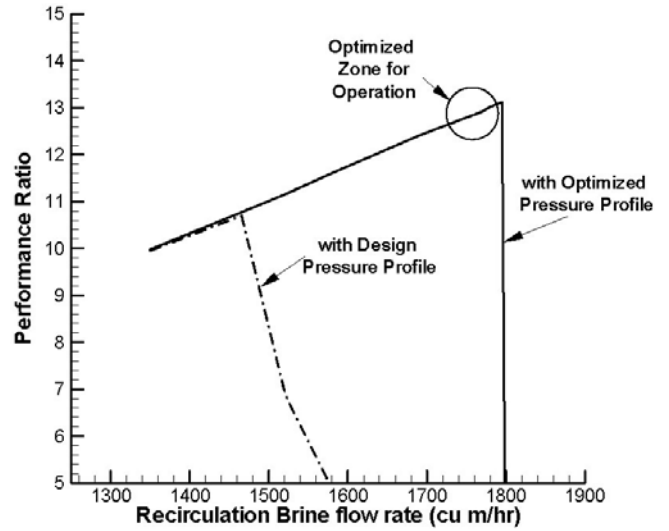
Fig. 21. Comparison of PR vs. RB flow rate for the design and optimized cases.

value. By optimizing the pressure profile there is an increase in the total LMTD of all stages.

i.e. $\sum_{i=1}^{39} LMTD$ which increases the value of TBT for a

given recirculation flow rate. In any MSF plant, the TBT keeps on decreasing with increasing RB flow rate. When the TBT is reduced below the first stage flashing temperature, there is no flashing in the first stage. This leads to a stoppage of flashing cascading to higher stages (second, third, etc.). Thus the PR drops suddenly as the RB flow rate crosses this threshold RB flow rate. Fig. 21 shows that the optimized pressure profile helps in increasing this threshold RB flow rate from 1,480 m³/h (with design pressure profile) to 1,795 m³/h (with optimized pressure profile). This increase in RB flow leads to higher value of PR of 13.12. At still higher RB flow rates the PR drops sharply due to non-flashing of stages. Thus, the stability of the plant around the optimum is also of equal concern. The operating optimum RB flow rate should be away from this "non-flashing cliff". The optimum RB flow rate should be chosen suitably far from this unstable location.

3.4. Changed scenarios in the NDDP MSF desalination plant and its optimization

An additional 20% RB tubes have been provided for two reasons, namely, (1) to adjust itself to the seasonal variation of seawater temperature and (2) to meet the extra demand for water whenever needed.

The entire zone of velocity of the RB flow rate from 1350 m³/h to 2000 m³/h and heat transfer area from
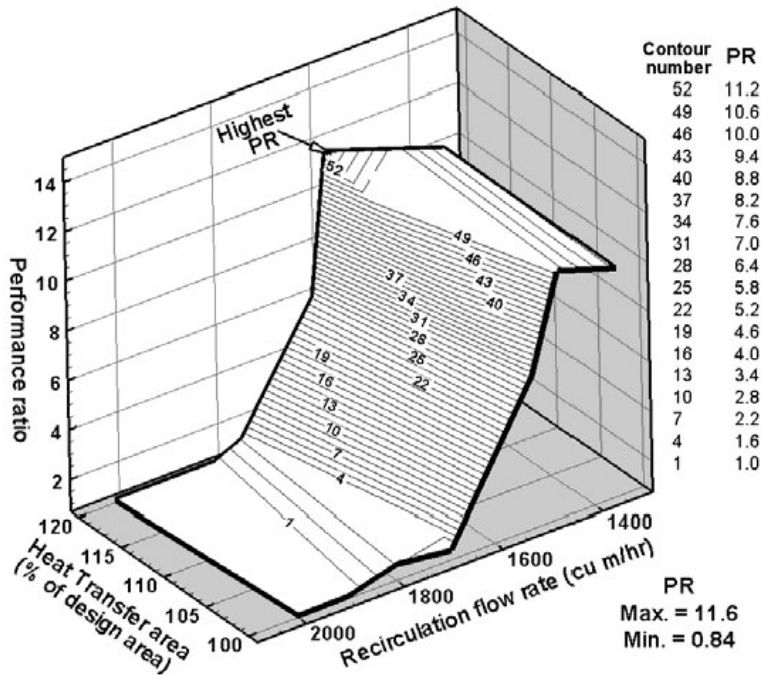
Fig. 22. PR as a function of heat transfer area and RB flow rate at design pressure conditions.
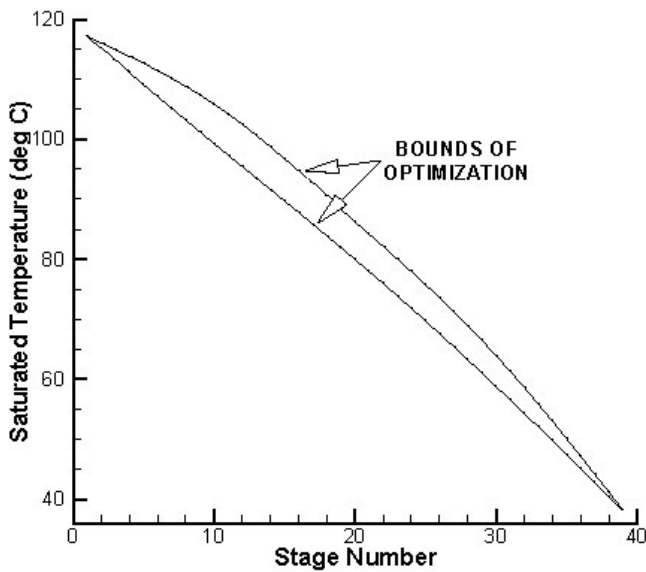
Fig. 23. Search space for the optimization of the pressure profile.
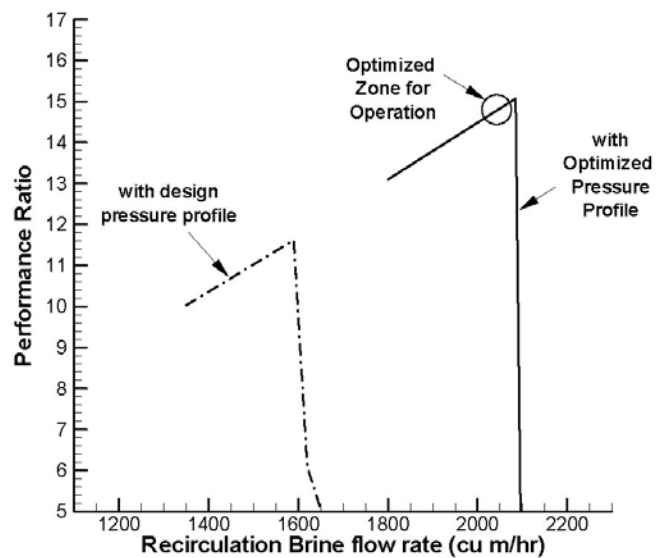
Fig. 24. PR as a function of RB flow rate, a comparison between design and optimized pressure profile (for an increased HT area case).

design value to the maximum available value, which is 20% excess of design value, has been scanned for evaluating the value of PR. This is shown as a contour plot in Fig. 22.

Thus an increase in area alone cannot increase the PR proportionately. A change in the operating heat transfer area always calls for an optimization study to decide the best operating conditions for the plant.

The details of the parameterization and the definition of objective function remain the same. However, the limits of optimization have been changed. The region in the vicinity (±4% to ±5%) of the optimum already obtained is chosen as our new design space as shown in Fig. 23. The initial conditions used was the optimum obtained in Section 3.3.

Fig. 24 gives the change in PR with the RB flow rate. A comparison of design and optimized pressure profile conditions are clearly shown. The GA-based optimizer converges to an optimum in 19 generations; the details of
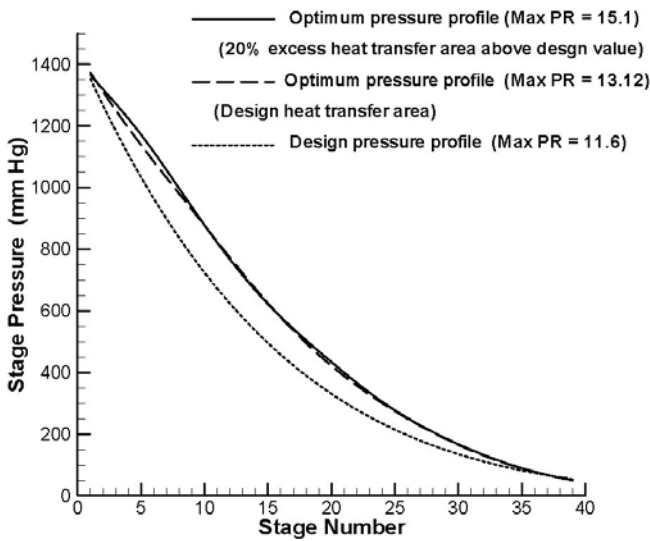
Fig. 25. Optimized pressure profiles in comparison with design pressure profile.

the optimum are given in Table 9. A PR of 15.1 is obtained with our new optimized pressure profile when the recirculation flow rate is 2,085 m³/hr. Fig. 25 gives a comparison of optimized pressure profiles under design and 20% excess heat transfer area.

Fig. 24 shows a sharp drop in PR when the RB flow rate crosses a threshold value (explained earlier). Using the optimized pressure profile an increase in the threshold

Table 9
Details of the optimized steady solution

Description	Optimized at 120% design HT area
Capacity, m³/d	7,526–7,599
TBT, °C	120.10–120.11
RB flow rate, m³/h	2,065–2,085
Brine heater temp. rise, °C	4.4–4.9
Performance ratio	14.96–15.09
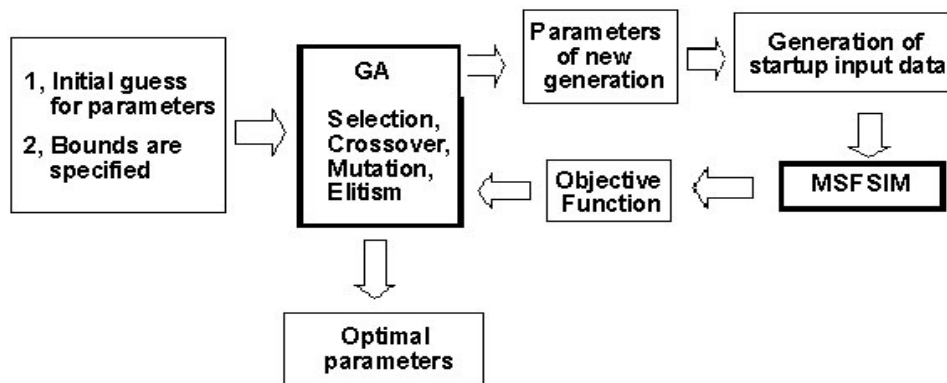
Fig. 26. Schematics showing the procedure of the coupled MSFSIM with GA.

Table 10
Parameterization of the start-up problem

Parameter	Initial range
Recirculating brine flow rate transient parameters	
CP_1 (time after which RB flow rate increases from its initial value), min	30–80
CP_2 (time after which RB flow rate reaches to its final value), min	200–500
CP_3 (initial RB flow rate), m³/h	200–500
CP_4 [variation over the mean value at time = $CP_1 + (CP_2 - CP_1)/3$]	0.6–1.4 times mean value
CP_5 [variation over the mean value at time = $CP_1 + (CP_2 - CP_1)*2/3$]	0.6–1.4 times mean value
CP_6 (final RB flow rate), m³/h	2,000–2,100
Pressure profile transient parameters	
CP_7 (minimum pressure the first stage attains during the start-up), mm Hg	500–700
CP_8 (time at which pressure profile starts recovering from its dip), min	60–200
CP_9 (time at which pressure profile attains its final values), min	120–300

RB flow rate from 1580 m^3/h to 2090 m^3/h was possible. This increase in RB flow leads to higher value of PR 15.1.

The optimized zone (shown in Figs. 21 and 24) has to be selected as per the controllability of the process and the instrumentation. This zone has to be sufficiently far from the sharp drop based on final operational considerations. In this paper we have studied the maximum theoretically achievable values.

4. Start-up optimization using GA

A steady-state optimum solution for NDDP MSF plant has been obtained in Section 3. The difficult question that arises is how to attain this optimum with an appropriate start-up. This requires a new optimization study to be performed, which regulates the shape of the recirculation flow transient and the pressure transient. Fig. 26 shows a schematic of the procedure adopted while coupling MSFSIM with GA for start-up optimization. Our objective was to optimize the recirculation transient and pressure transient during start-up so that it reaches the stable optimum.

The objective function (OF) to be maximized is chosen such that it reaches the value of PR = 15.0 (steady-state optimum) in a minimum amount of time

$$OF = 300 \left[\frac{e^{-\text{Max}\,(|PR-15|,\,P_{tol})}}{N_t} \right]$$

where PR is the performance ratio and N_t is the time taken for the production to stabilize.

The objective function chosen enforces a penalty for not reaching PR = 15.0. This penalty function approach brings about faster convergence [13]. $P_{tol} = 0.2$ is the tolerance allowed, i.e. an under-optimized PR should reach a value within 14.8 to 15.2. The factor of 300 is to make the value of OF approach unity on convergence. This would make the convergence faster [12].

4.1. Parameterization of the problem

Nine control parameters were chosen for this problem. Of these, six parameters are used for representing the recirculating brine flow control with respect to start-up (Fig. 27). Three parameters were used for stage pressure control so that the pressure transient can be controlled as a whole. The pressure transient parameterization is shown in Fig. 28. The start-up pressure profile saturates to the values of the optimized pressure profile obtained in Section 3. The initial range of optimization for these parameters is given in Table 10.
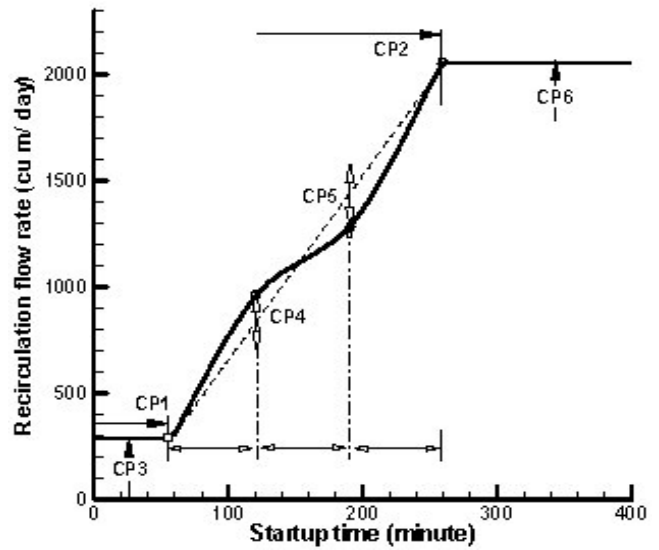
Fig. 27. Parameterization of the recirculation curve.
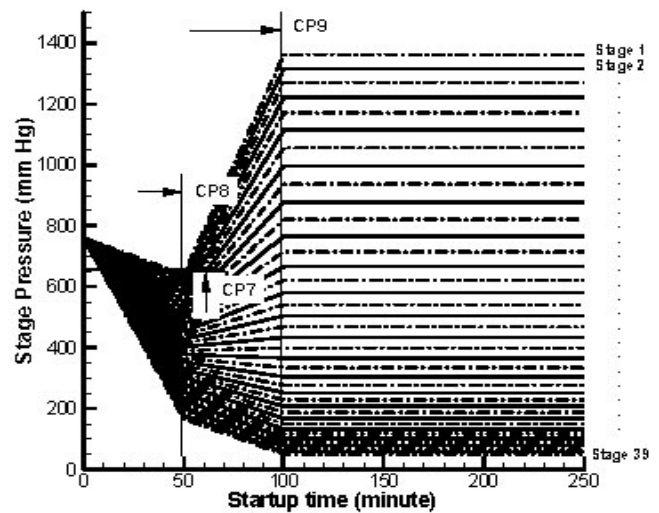
Fig. 28. Parameterization of the start-up pressure profile.

Table 11
Details of the optimized parameters

Control parameter	Final optimized values
CP_1, min	58
CP_2, min	258
CP_3, m^3/h	286
CP_4	1.15 times mean value
CP_5	1.1 times mean value
CP_6, m^3/h	2055
CP_7, mm Hg	603
CP_8, min	55
CP_9	107
Time to reach the desired production rate	265
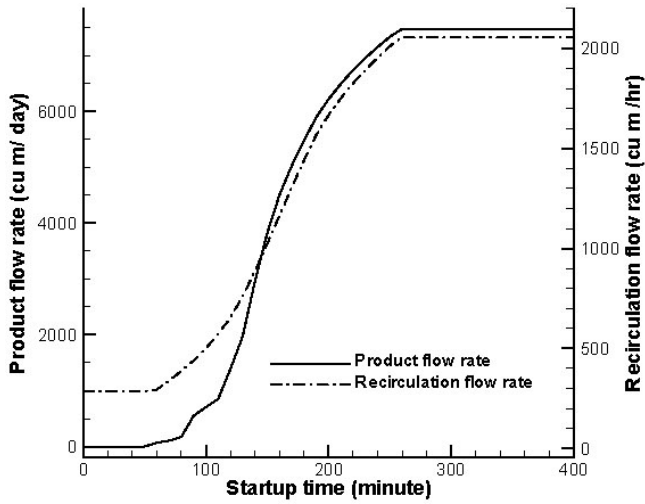
Fig. 29. Optimized recirculation curve and its corresponding production curve.
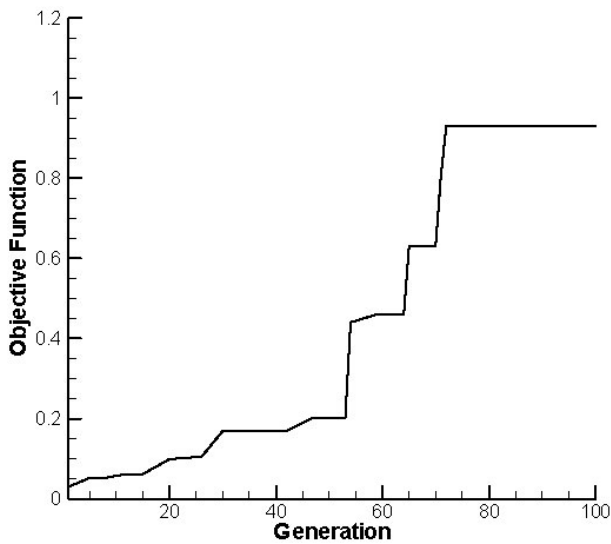
Fig. 30. Evolution of objective function with generation.

Fig. 31. Final optimized pressure transient.

Fig. 32. Optimized feed, reject and blow-down rates during start-up.

4.2. Results of start-up optimization (target PR = 15.1)

Table 5 gives the details fixing the parameters within GA. Fig. 30 gives the evolution of the objective function with the generation. The saturation in objective function is attained after 72 generations.

The optimized sets of parameters are given in Table 11. Fig. 29 gives the optimized recirculation flow rate and production rate as function of startup time. Fig. 31 shows the final optimized pressure transient. Fig. 32 gives the feed, reject and blow down flow rates during start-up under the optimum condition. The desired steady-state optimum production rate could be reached in a minimum amount of 265 min (see Fig. 29).

5. Future scope

The state space formulation of the MSF system can be shown as $\dot{\vec{y}} = J\vec{y} + \vec{q}$. If the vector $\vec{q}$ due to the non-linear terms is neglected, it becomes $\dot{\vec{y}} = J\vec{y}$. Here, $\vec{y}$ is the vector space due to deviations from the steady-state value of variables like performance ratio, recirculation flow rate, distillate production rate, steam mass flow rate, etc. defined as $\vec{y} = \vec{x}_i - \vec{x}_{i,\text{steady state}}$. $\dot{\vec{y}}$ is the rate of change of state variable

$$\left[\frac{\partial y_1}{\partial t} \quad \frac{\partial y_2}{\partial t} \quad \cdots \quad \frac{\partial y_n}{\partial t} \right]^T$$

J is the Jacobian matrix which can be generated by the MSFSIM code. In future work, the Jacobian matrix J based on NDDP MSF will be coupled with the control systems.

6. Conclusions

MSFSIM, a simulator for desalination process, was developed and extensively validated with pilot plant data. MSFSIM has been used for the simulation of an NDDP MSF plant which is under construction at Kalpakkam, India. The most important parameter in the MSF plant, i.e., the stage-wise pressure profile and recirculation flow rate, have been optimized. A substantial increase in the performance ratio from design value to 15.1 (stable optimized value) was obtained. This optimization was aimed at minimizing the time for start-up as the plant evolves to the optimized PR, i.e., 15.1.

7. Symbols

A_i	—	Outer surface area of all tubes in stage i, m^2
C_B	—	Specific heat of brine, J/kg K
C_W	—	Specific heat of water, J/kg K
C_T	—	Specific heat of tube material, J/kg K
$d_i, d_o, \bar{d}_T$	—	Inner, outer and log mean diameter of the recirculating tubes, m
EBP	—	Elevation in boiling point, K
E_L	—	Enthalpy of saturated liquid, J/kg
E_S	—	Enthalpy of saturated steam, J/kg
f_i	—	Flashing in stage i, m^3/h
g	—	Gravitational constant, m/s^2
h_i, h_o	—	Heat transfer coefficient inside and outside recirculating tubes, W/m^2 K
J	—	Jacobian matrix
k_B, k_W	—	Thermal conductivity of the brine and recirculating tube, W/m K
L	—	Length of the tube, m
n	—	Number of stages
N_t	—	Time required for start-up, s
P_i	—	Pressure in stage i, mm Hg
S_{BD}	—	Blow-down salinity
t	—	Time, s
$T_{B,i},$ $T_{B,i+1}$	—	Inlet and outlet brine temperature of stage i, K
T_C	—	Recirculating brine temperature, K
$T_{Sat,i}$	—	Saturation temperature for water in stage i, K
T_W	—	Tube wall temperature, K
U_O	—	Overall heat transfer coefficient, W/m^2 K
V	—	Velocity of brine inside the tube, m/s
$V_{RB,Max}$	—	Maximum velocity in the recirculating brine, m/s

W_S	—	Steam flow rate in brine heater, kg/s
$W_{O,i}$	—	Brine hold-up in evaporator stage i, kg
$W_{P,i}$	—	Water flow rate in the distillate corridor stage i, kg/s
W_{Di}	—	Re-flashing vapor rate from stage i, kg/s
W_{Fi}	—	Flashing vapor flow rate from stage i, kg/s
W_{RSi}	—	Brine hold-up inside tubes in stage i, kg
$W_{R,i},$ $W_{R,i+1}$	—	Inlet and outlet brine flow rate of stage i, kg/s
W_T	—	Weight of tubes per stage, kg
$[\ ]^T$	—	Transpose of a vector

Greek

α, β	—	Weights of objective functions
κ	—	Coefficient of heat loss
λ_b	—	Latent heat of recirculating brine, J/kg
λ_w	—	Latent heat of product water, J/kg
μ_B, μ_W	—	Viscosity of brine at brine temperature and wall temperature, kg/m K
σ	—	Average variation of the flashing rate in all stages, m^3/h

References

[1] G.N. Sashi Kumar, M. Chatterjee, A.K. Mahendra, P.K. Tewari, V.D. Puranik and G. Gouthaman, in: Advances in Separation Processes, Allied Publishers, 2005, pp. 181–190.
[2] International Atomic Energy Agency, TECDOC 1056, Vienna, 1998.
[3] M. Chatterjee, G.N. Sashi Kumar, A.K. Mahendra, V.D. Puranik, P.K. Tewari and G. Gouthaman, Proc. CHEMCON, Hyderabad, India, 2002.
[4] M. Chatterjee, G.N. Sashi Kumar, A.K. Mahendra, A. Sanyal and G. Gouthaman, NDDP multi-stage flash desalination process simulator design (Part 1), BARC Report, BARC/2006/E/011, 2006.
[5] G.N. Sashi Kumar, A.K. Mahendra, M. Chatterjee, A. Sanyal and G. Gouthaman, NDDP multi-stage flash desalination process simulator design (Part 2), start-up and optimization, BARC report, in press.
[6] M.A. Darwish, M.M. El-Rafaee and M. Abdel-Jawad, Desalination, 100 (1995) 35–64.
[7] P. Fiorini and E. Sciubba, Desalination, 136 (2001) 177–188.
[8] R.K. Verma, Technical aspects of coupling a 6300 m^3/d MSF–RO desalination plant to a PHWR, International Atomic Energy Agency, TECDOC 1056, Vienna, 1998.
[9] R.L. Haupt and S.E. Haupt, Practical Genetic Algorithms, Wiley-Interscience, New York, 2004.
[10] A.K. Mahendra, A. Sanyal and G. Gouthaman, GA based optimization of process network, Internal Report, MDD, BARC, 2003.

[11] G.N. Sashi Kumar, A.K. Mahendra and S.M. Deshpande, Optimization of airfoil shape using genetic algorithm and grid free solver, Proc. 7th Aeronautical Society of India, CFD International Conference, Bangalore, India, 2004.
[12] G.N. Sashi Kumar, Shape optimization using a meshless flow solver and modern optimization techniques. MSc (Engg.) Thesis, Department of Aerospace Engineering, Indian Institute of Science, Bangalore, 2006.
[13] G.N. Sashi Kumar, A.K. Mahendra and S.M. Deshpande, Optimi-
zation using genetic algorithm and grid-free CFD solver, CFD J., 16(4) (2008) 425–433.
[14] G.N. Sashi Kumar, A.K. Mahendra and S.V. Raghurama Rao, AIAA paper No. 2007-3830, 18th AIAA-CFD Conference, Miami, FL, 2007.
[15] W.L. McCabe and J.C. Smith, Unit Operations of Chemical Engineering, 6th ed., McGraw-Hill Higher Education, Singapore, 2001.
[16] H.E. Homig, Fichtner Handbook, Vulkan, Essen, 1978.

Appendix A

A.1. Model equations for MSF plant simulation

- Heat balance for tube in brine heater:

$$\frac{\mathrm{d}T_{w,i}}{\mathrm{d}t} = \kappa\left(\Delta E_{S,BH}\right) - \Delta\tilde{T} \tag{A1}$$

where

$$\Delta E_{S,BH} = \frac{W_S\left(E_S - E_L\right)}{C_T W_T} \qquad \text{and}$$

$$\Delta\tilde{T} = \frac{U_{O,i} A_i\left[T_{W,i} - 0.5\left(T_{C,i} + T_{B,i}\right)\right]}{C_T W_T}$$

- Heat balance for brine in brine heater:

$$\frac{\mathrm{d}T_{B,i}}{\mathrm{d}t} = \kappa\left(\Delta\tilde{T}_B\right) - \Delta\tilde{T}_C \tag{A2}$$

where

$$\Delta\tilde{T}_B = \frac{U_{o,i} A_i\left[T_{W,i} - 0.5\left(T_{C,i} + T_{B,i}\right)\right]}{C_B W_{RS,i}}$$

and

$$\Delta\tilde{T}_C = \frac{W_{R,i}\left(T_{B,i} - T_{C,i}\right)}{W_{RS,i}}$$

- Heat balance for coolant in evaporator:

$$\frac{\mathrm{d}T_{C,i}}{\mathrm{d}t} = \phi T_{W,i+1} - \left(\frac{\phi}{2} - \varphi\right)T_{C,i} + \varphi T_{C,i+1} \tag{A3}$$

where

$$\phi = \frac{U_{O,i+1} A_{i+1}}{C_{B,i} W_{RS,i+1}}, \quad \varphi = \frac{W_{R,i}}{W_{RS,i+1}}$$

- Heat balance for vapor in evaporator:

$$\frac{\mathrm{d}T_{W,i+1}}{\mathrm{d}t} = \eta\left(E_{S,i} - E_{L,i}\right)$$
$$-\gamma\left(T_{W,i+1} - \frac{T_{C,i} + T_{C,i+1}}{2}\right) \tag{A4}$$

where

$$\eta = \frac{\kappa\left(W_{F,i} + W_{D,i}\right)}{C_T W_{T,i+1}}, \quad \gamma = \frac{U_{O,i+1} A_{i+1}}{C_T W_{T,i+1}}$$

- Heat balance for brine in evaporator:
-

$$\frac{\mathrm{d}T_{B,i+1}}{\mathrm{d}t} = \frac{W_{R,i} T_{B,i} - W_{R,i+1} T_{B,i+1}}{W_{O,i}} = \frac{W_{F,i} E_{S,i+1}}{C_B W_{O,i}} \tag{A5}$$

where

$$W_{F,i} = \frac{W_{R,i} C_{B,i}\left(T_{B,i} - T_{sat,i} - EBP\right)}{\lambda_B} \tag{A6}$$

$$W_{D,i} = \frac{W_{P,i} C_{W,i}\left(T_{sat,i-1} - T_{sat,i}\right)}{\lambda_W} \tag{A7}$$

$$W_{R,i+1} = W_{R,i} - W_{F,i} \tag{A8}$$

$$W_{P,i+1} = W_{P,i} + W_{F,i} \tag{A9}$$

$$\frac{1}{U_o} = \frac{d_o}{d_i}\frac{1}{h_i} + \frac{(d_o - d_i)/2}{\bar{d}_t}\frac{d_o}{k_w} + \frac{1}{h_o} + FF \tag{A10}$$

FF is the fouling factor which is taken to be between 0.09 to 0.15 m^2K/kW (time dependent) for the evaporators and where as for the brine heater this value is taken as 0.25 m^2K/kW. Selection of such high design fouling factors for the MSF plants allows these plants to operate at a TBT equal to or even higher than maximum design values. This results in higher productivity.

The vapor side film heat transfer coefficient, h_o, [15] is given by the Nusselt equation:

$$h_o = 0.729 \times \left(\frac{k_B^3 \cdot g \cdot \rho_B^2}{d_o \cdot \Delta T \cdot N \cdot \mu_B}\right)^{0.25} \left(E_S - E_S\right)^{0.25} \tag{A11}$$

$$\Delta T = T_{vapor} - 0.75\left(T_{vapor} - T_{wall}\right) \tag{A12}$$

where N is the number of horizontal tubes in the stack, and the brine side convective heat transfer coefficient, h_i [15], is given by the Sieder–Tate equation:

$$h_i = 0.027$$

$$\times \frac{k_B}{d_i}\left(\frac{d_i \cdot V \cdot \rho_B}{\mu_B}\right)^{0.8}\left(\frac{C_B \cdot \mu_B}{k_B}\right)^{0.33}\left(\frac{\mu}{\mu_w}\right)^{0.14}$$

(Re >10,000) \hfill (A13)

For A_i, $T_{B,i}$, $T_{C,i}$, $T_{BW,i}$, $W_{RS,i}$ and $U_{o,i}$ where $i = 1$ corresponds to the brine heater and $i = 2$–40 correspond to stages 1–39. For $W_{F,i}$, $W_{D,i}$, $W_{P,i}$ $i = 1$–39 corresponds to stages 1–39.

A.2. Correlations for physical properties of brine [16]

1. Density:

- Validity: Salinity (S) = 0–160 g/kg
  (i.e. 0–160,000 ppm)
- Temperature (T) = 10–180°C

Density (g/cm^3) = $0.5\, a_0 + a_1\,(Y) + a_2(2Y^2 - 1)$
$$+ a_3(4Y^3 - 3Y) \tag{A14}$$

where $Y = (2T - 200)/160$

$a_0 = 2.016110 + 0.115313X + 0.000326\,(2X^2 - 1)$
$a_1 = -0.05410 + 0.001571X - 0.000423\,(2X^2 - 1)$
$a_2 = -0.006124 + 0.001740X - 0.000009\,(2X^2 - 1)$
$a_3 = 0.000346 + 0.000087X - 0.000053\,(2X^2 - 1)$

and $X = (2S - 150)/150$

2. Viscosity:

- Validity: Salinity (S) = 0–130 g/kg
  (i.e. 0–130,000 ppm)
- Temperature (T) = 10–150°C

Viscosity (cP) = $N_W * N_R$
Viscosity of pure water:
$\quad N_W = \exp\left[-3.79418 + 6047.129/(139.18 + T)\right]$ \hfill (A15)
Relative viscosity:
$\quad N_R = 1 + a_1\,S + a_2\,S^2$

where

$a_1 = 1.474*10^{-3} + 1.5*10^{-5}T - 3.927*10^{-8}\,T^2$
$a_2 = 1.0734*10^{-5} - 8.5*10^{-8}T + 2.23*10^{-10}\,T^2$

3. Thermal conductivity:

- Validity: Salinity (S) = 0–100 g/kg
  (i.e. 0–100,000 ppm)
- Temperature (T) = 10–150°C

Thermal conductivity (W/m.K) = $10^{-3}*$
$$(a_0 + a_1\,T + a_2\,T^2) \tag{A16}$$

$a_0 = 576.6 - 34.64X + 7.286X^2$
$a_1 = (1526 + 466.2X - 226.8X^2 + 28.67X^3)*10^{-3}$
$a_2 = -(581 + 2055X - 991.6X^2 + 146.4X^3)*10^{-5}$
and $X = 28.17S/(1000 - S)$

4. Specific heat capacity

- Validity: Salinity (S) = 0–160 g/kg
  (i.e. 0–160,000 ppm)
- Temperature (T) = 0–180°C

Specific heat (J/kg.K) = $a_0 + a_1\,T + a_2\,T^2 + a_3\,T^3$

\hfill (A17)

$a_0 = 4206.8 - 6.6197S + 1.2288*10^{-2}\,S^2$
$a_1 = -1.1262 + 5.4178*10^{-2}S - 2.2719*10^{-4}\,S^2$
$a_2 = 1.2026*10^{-2} - 5.356*10^{-4}S + 1.8906*10^{-6}\,S^2$
$a_3 = 6.8774*10^{-7} + 1.517*10-6\,S - 4.4268*10^{-9}\,S^2$

Specific enthalpy (kcal/kg) = h_o + 2.38846*10^{-4}

$\quad$ *(a_0 + a_1 T + a_2 T^2 + a_3 T^3)$\qquad\qquad$ (A18)

where h_o = 2.3*10^{-3}S – 1.03*10^{-4} S^2

5. Boiling point elevation:

- Validity: Salinity (S) = 20–160 g/kg
  $\qquad\qquad$ (i.e. 0–160,000 ppm)
- Temperature (T) = 20–180°C

Boiling point elevation (BPE) (K) = S (a_0 + a_1 S)$\quad$ (A19)

a_0 = (6.71 + 6.43*10^{-2}T + 9.74*10^{-5} T^2)*10^{-3}

a_1 = (22.38 + 9.59*10^{-3}T + 9.42*10^{-5} T^2)*10^{-5}

6. Vapor pressure:

- Validity: Salinity (S) = 0–160 g/kg
  $\qquad\qquad$ (i.e. 0–160,000 ppm)

Vapor pressure (bar) = P_w (1 – 0.000537S)$\qquad$ (A20)

where P_w is the vapor pressure of pure water at a given temperature.